DesignCon 2019

Insertion Loss vs. Integrated Crosstalk Noise Metric for Link Analysis

Shayan Shahramian, Huawei Canada – HiLink,
shayan.shahramian@huawei.com

Hossein Shakiba, Huawei Canada, HiLink

Behzad Dehlaghi, Huawei Canada - HiLink

David Cassan, Huawei Canada - HiLink

Davide Tonietto, Huawei Canada - HiLink

Abstract:

There is a growing trend in industry to characterize high-speed links in terms of their integrated crosstalk noise (ICN) tolerance at different insertion losses. The slope of the insertion loss vs. ICN plot (typically in dB/mV) is now becoming one of the key metrics to evaluate and compare the performance across different systems. In this paper, a mathematical analysis and simulation methodology is presented on how to calculate the total ICN which can be tolerated in the presence of other impairments such as thermal noise, residual ISI, and timing jitter. The accuracy of the mathematical analysis is confirmed by statistical simulations.

Author Biographies:

Shayan Shahramian received his Ph.D. from the Department of Electrical and Computer Engineering at the University of Toronto, Canada, in 2016. His focus is on high-speed chip-to-chip communication for wireline applications. He is the recipient of the NSERC Industrial Postgraduate scholarship in collaboration with Semtech Corporation (Gennum Products). He is the recipient of the best young scientist paper award at ESSCIRC 2014 and received the Analog Devices outstanding designer award for 2014. He joined Huawei Canada in January 2016 and is currently working in system/circuit level design of high-speed energy-efficient transceivers for short reach applications.

Hossein Shakiba received his B.Sc. and M.Sc. degrees in Electrical Engineering from the Department of Electrical and Computer Engineering at the Isfahan University of Technology, Iran, in 1985 and 1989, respectively, and his Ph.D. degree in Electrical Engineering from the Department of Electrical and Computer Engineering at the University of Toronto, Canada, in 1997. He has over 30 years of teaching, research, design, and management experience in the area of analog circuit and system design for various applications with focus on wireline communication in both the industry and academia. He is currently working on system and circuit design and development for next generation short reach and high efficiency serial links at Huawei Canada.

Behzad Dehlaghi received the B.Sc. degree from University of Tehran, Tehran, Iran, in 2009, and the M.Sc. degree from University of Calgary, AB, Canada, in 2012, both in electrical engineering. He completed the Ph.D. degree in electronics at the University of Toronto, Toronto, ON, Canada in 2017. During his Ph.D. he worked on parallel ultra-short reach die-to-die links. Since January 2016 he has been working at Huawei Canada where he is involved in the system/circuit level design of energy-efficient high-speed transceivers. His research interests include on-chip measurement circuits and high-speed chip-to-chip communication.

David Cassan received the M.A.Sc degree in Electrical Engineering from the University of Toronto in 2001. He is currently working at Huawei Canada where he is leading the High-Speed Interfaces Research Team in Toronto. He has more than 15 years of experience in the area of wireline transceivers including analog design, system design, and SI/PI analysis. Previously he was a Director of Engineering at Snowbush IP where he led several generations of their wireline transceiver developments. His research interests include high efficiency and short reach transceiver designs for both electrical and optical applications.

Davide Tonietto received his Laurea Degree in 1995 from University of Pavia, Italy. Currently he is the Director of SerDes Development at Huawei Canada Research Center, Ottawa. He has more than 15 years of experience in signal integrity and high speed serial interface design and development. Previously he was Senior Manager of Signal Integrity IC development at Gennum Corporation, Manager of SerDes IP development at STMicroelectronics and lead designer of high speed serial interfaces, at Broadcom and other companies.

I. Introduction

In high-speed link design, data is transmitted over a channel with impairments that degrade the signal quality. Usually the key impairments are insertion loss (IL) and crosstalk. There is a growing trend in industry to characterize high-speed links in terms of their integrated crosstalk noise (ICN) tolerance at different insertion losses (e.g. for different channels). The slope of the ICN vs. IL plot (typically in dB/mV) is now becoming one of the key metrics to evaluate and compare the performance (e.g. bit-error rate (BER)) across different systems. This slope simply quantifies the amount of IL that is needed to be changed in response to a change in the crosstalk to keep the same performance. Equivalently, the slope indicates how much change in the crosstalk is needed to keep the performance similar if the link IL changes.

The analysis in this paper helps derive information for when different impairments begin to dominate the link performance. In many cases, after the effect of inter-symbol interference (ISI) is removed by equalization, ICN dominates the performance. Therefore, the total amount of ICN that can be tolerated given a specific IL becomes an important criteria. The analysis results in an ICN vs. IL plot which can be used to derive the IL vs. ICN slope metric. Figure 1 shows an example ICN vs. IL curve and a plot of the IL vs. ICN slope. As expected, the total amount of ICN that can be tolerated decreases as the IL increases. The typical trend in slope is that at lower IL, there is a lower IL vs ICN slope (in dB/mV) compared to higher IL. The main interpretation is that at lower loss, for a small increase in the loss, there is a large degradation in the maximum amount of tolerable ICN. On the other hand, at higher losses, for a large increase in the loss, only a small change in the tolerable ICN is observed. The main goal of this paper is to provide a methodology to determine the IL vs. ICN slope for a given link and to understand the overall system sensitivity to crosstalk and IL.

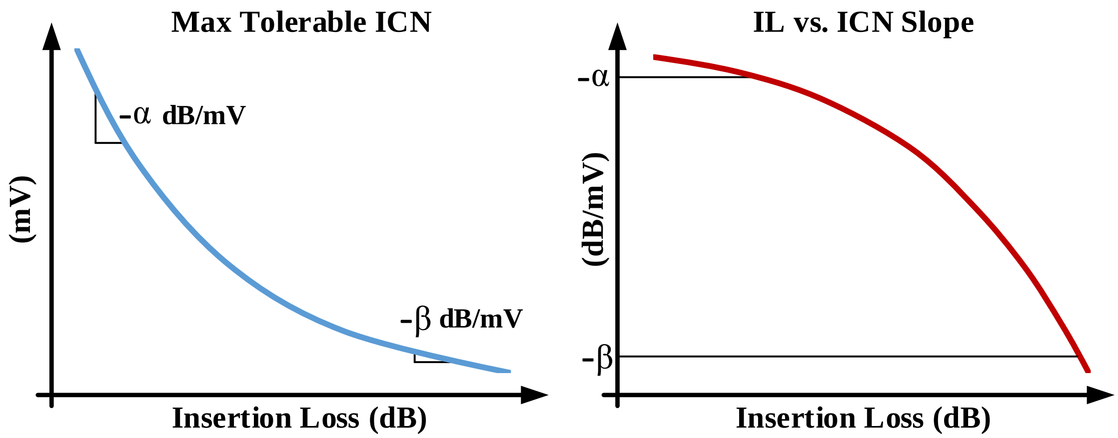

Figure 1 - (left) maximum tolerable ICN vs. IL, (right) IL vs. ICN slope

Intuitively, it is expected that at lower insertion losses, the system can handle more ICN due to the larger eye opening and the additional margin. However, it is also desirable to understand why the slope of the IL vs. ICN changes with the amount of IL. To explain this intuitively, one can initially assume that the system is purely crosstalk limited and that all of the ISI is cancelled perfectly. In such a system, the main cursor amplitude of the pulse response will determine the eye opening and as a result the margin that exists for crosstalk. Figure 2 shows channel insertion losses between 10-12dB and 34-36dB (at the Nyquist frequency of 15GHz) and the corresponding pulse response for each case. The pulse response peak drops by ~5% for each additional dB increase in the channel loss. This leads to larger drops in the absolute value of the pulse response for lower losses and a smaller amount for higher losses as can be seen in Figure 2. As a result, at lower losses, a small increase in loss leads to a larger reduction in eye opening which will degrade the ICN tolerance by a larger amount. At higher losses, the additional dB of loss, leads to a very small impact on the main cursor amplitude and as a result will have a smaller impact on the ICN tolerance. This explanation is for a system that has all ISI removed and is only crosstalk limited. In practice, different impairments in the system affect the tolerable ICN as well as the IL vs. ICN slope and are discussed in section III.

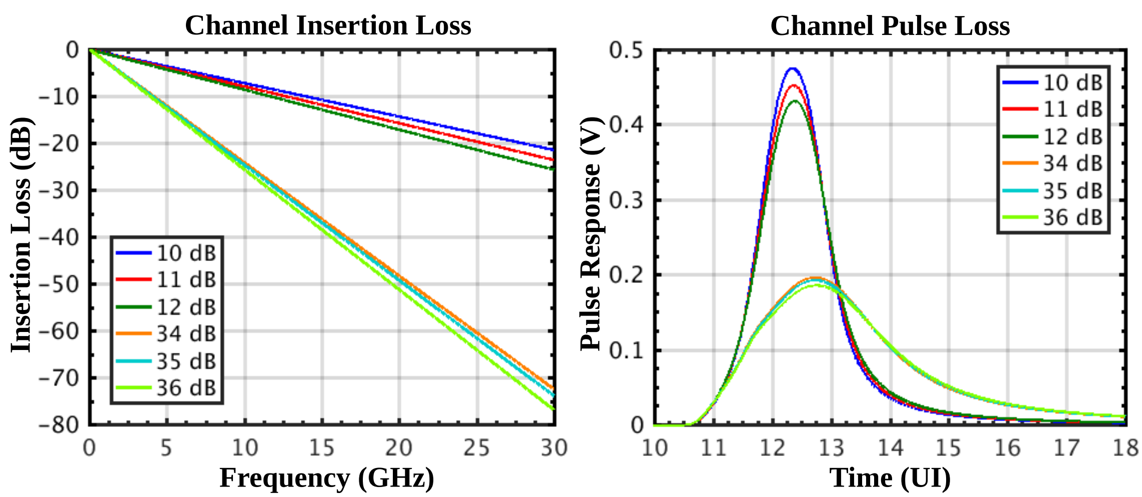

Figure 2 – IL vs frequency scaled to obtain different losses and the pulse response corresponding to each channel IL (Insertion loss numbers are reported at the Nyquist frequency of 15GHz)

One important aspect of ICN tolerance is the point in the overall link where ICN is calculated. Section II.A discusses the trade-offs between calculating the ICN at the receiver package ball vs the receiver silicon die bump. Section II.B outlines different methodologies that can be used to determine the amount of ICN present in a given link. These two methodologies include a frequency and a time domain method. Both approaches are discussed along with their advantages and disadvantages.

The remainder of the paper provides a mathematical analysis and simulation methodology on how to calculate the total ICN which can be tolerated in the presence of other impairments such as thermal noise, residual ISI, and timing jitter. The accuracy of the mathematical analysis is confirmed by statistical simulations. The mathematical analysis is provided in section III while the simulation results are provided in section IV.

II. ICN Calculation

For a given link, to quantify ICN, two important decisions need to be made. The first decision is at what point in the overall link will the ICN will be referenced to and is discussed in section II.A. The second decision is regarding the method to calculate ICN which is outlined in section II.B.

A. ICN at Package Ball vs. Die Bump

IL is typically reported from the transmitter die bump to the receiver die bump (bump-to-bump) as a function of frequency and is usually represented by its value at the Nyquist frequency. IL causes dispersion which leads to ISI. To quantify ICN, the crosstalk impairment needs to be referenced to a specific point along the link. Although many standards specify ICN at the ball of the receiver package (OIF-CEI-56G-VSR-PAM4, IEEE 400GAUI-8-C2M, etc), calculating ICN at the receiver bump is also important for a more complete link performance analysis. Figure 3 shows a link comprising of a transmitter die inside a package connected to a receiver package through PCBs and a connector. In Figure 3(top) the receiver package ball is chosen as the reference point for ICN. When ICN is referred to the ball, the crosstalk in the receiver package will not be considered in the ICN value. Figure 3(bottom) depicts which point in the link would be considered if the ICN is referred to the bump. Each method has its own advantages and disadvantages as summarized in Table 1.

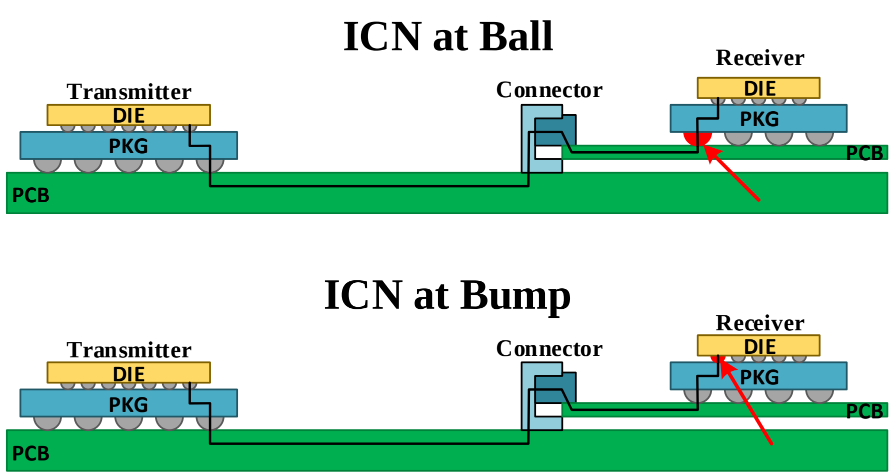

Figure 3 - A link comprised of a transmitter die/package connected to a receiver die/package through a PCB and a connector

One of the reasons to refer the crosstalk to the receiver ball is to be able to correlate the results with measurements. It is easier to infer the crosstalk at the ball rather than the bump, since the crosstalk at the bump would require details of the receiver package, a node not easily observable. Secondly, if the ICN is referred to the ball, it makes it easier to compare receiver performance across different vendors. The receiver package design would then be eliminated in the calculation and the overall link performance would be determined for a given amount of ICN at the ball. For this reason, standards report the ICN at the ball and in order to show standard compliance, it is also required to report the tolerable ICN at the ball. The main downside of reporting ICN at the ball is that it does not capture the impact of the receiver package. When optimizing the overall link, it can become critical to know the effect of the receiver package on performance. Referring the crosstalk to the bump allows for the entire crosstalk impact to be captured. If the receiver package has poor crosstalk performance, this will show up as a larger ICN at the receiver bump. Unfortunately, as mentioned earlier, it is difficult to measure the ICN at the bump and to correlate the calculations/simulations to measurements. Therefore, the best approach is to calculate the ICN of the link *both* at the ball and bump. Looking at ICN at both the bump and ball, can help guide where to put more effort in the optimization of the package design. For the remainder of the paper, it is assumed that the package design has been finalized and only the ICN tolerance relative to the standard is required. Therefore, ICN at the ball will be used to show the methodology. However, the same analysis can be applied using the ICN at the bump.

Table 1 - Summary of advantages/disadvantages of referring ICN to Ball vs bump

ICN at Ball	ICN at Bump
Can be correlated to measurements	Captures entire link crosstalk impact
Allows comparison to other vendors	Difficult to measure
Standards quote ICN at ball	
Does not capture RX package impact	

B. Frequency Domain vs. Time Domain

There are two different ways to calculate ICN for a given link. One approach is using a frequency domain method where the power spectral density (PSD) of the received signal due to all aggressors is integrated across the entire frequency range to obtain a root-mean square (RMS) value. The PSD of the received crosstalk signal can be calculated from the PSD of the transmitted aggressors and the channel crosstalk responses. In the second approach, the pulse response of the receiver due to all crosstalk paths in the time domain is used to quantify ICN. The pulse response is sampled and used to generate a probability density function (PDF) which can then be used to calculate the RMS value.

Figure 4 shows an example with two aggressors with identical transmitter power spectral densities, $TX_{PSD}(f)$, and two different crosstalk transfer functions, $H_{X,1}(f)$ and $H_{X,2}(f)$. The different crosstalk transfer functions will be square summed and used to determine the ICN.

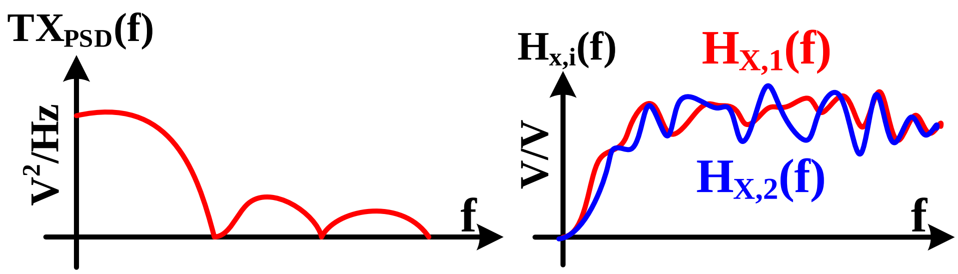

Figure 4 - (left) Sample power spectral density of the transmitter (right) example transfer functions for different crosstalk aggressors

To calculate ICN using the frequency domain method the following equation can be used:

$$ICN = \sqrt{\int_{-\infty}^{\infty} TX_{PSD}(f) \times \sum_i \left|H_{X,i}(f)\right|^2 df} \quad (1)$$

The details for calculating $TX_{PSD}(f)$ are provided in Section III. Using the frequency domain method allows for the ICN to be quickly calculated from the s-parameters. This is also the method that is commonly used by standards [1], therefore making comparisons easier. However, this may not represent the impact of the actual crosstalk. Intuitively, one can envision two different crosstalk frequency responses that when integrated will have the same ICN, however, the transient data through them can lead to different effects on the system performance.

To more accurately capture the impact of crosstalk on the link performance, a time domain approach can be used. In this approach, the inverse Fourier transform of the crosstalk channel is performed for each aggressor to obtain the impulse response.

$$I_i(t) = \mathcal{F}^{-1}\{H_{x,i}(f)\} \quad (2)$$

The impulse response can then be convolved with a lone pulse to obtain the pulse response of the crosstalk channel.

$$P_i(t) = (U(t) - U(t-T)) \circledast I_i(t) \quad (3)$$

Where U(t) is the unit step function and T is the baud-rate of the signal. The next step is to create a PDF of the crosstalk from the pulse response. In order to do this, the pulse responses need to be sampled at the baud-rate as sampling phase varies through a full unit interval (UI). For each chosen sampling phase, a PDF can be generated:

$$pdf_{i,M-PAM}(x,\zeta) = Conv_n\left(\frac{1}{M}\sum_{y=0}^{M-1} \delta\left(x - \left(\frac{2y}{M-1} - 1\right)\right) \times P_i(n+\zeta)T\right) \quad (4)$$

Where M refers to the number of pulse-amplitude modulation (PAM) levels, i is the crosstalk aggressor number, x represents the crosstalk voltage value, n signifies samples of the pulse response, ζ is the chosen sampling phase and should cover a full UI. Finally, the PDF needs to be averaged over all the different sampling phases ζ.

$$pdf_{i,M-PAM}(x) = \frac{1}{OSR} \sum_{\zeta=0}^{OSR-1} pdf_{i,M-PAM}(x,\zeta) \tag{5}$$

In the above equation OSR represents the oversampling ratio (number of samples per UI) of the pulse response. The ICN can then be calculated by square summing the RMS value of each aggressors' PDF.

$$ICN = \sum_{i} \left(\sqrt{\sum_{x} pdf_{i,M-PAM}(x) \times x^2} \right)^2 \tag{6}$$

A simple example of calculating the PDF of the crosstalk using an arbitrary pulse response is shown in Figure 3 for a case when M=2. Given a sampling phase, for each sample a PDF is created for that level of the pulse response. The PDFs are all convolved together to get the complete PDF for a given sampling phase as shown in equation (4).

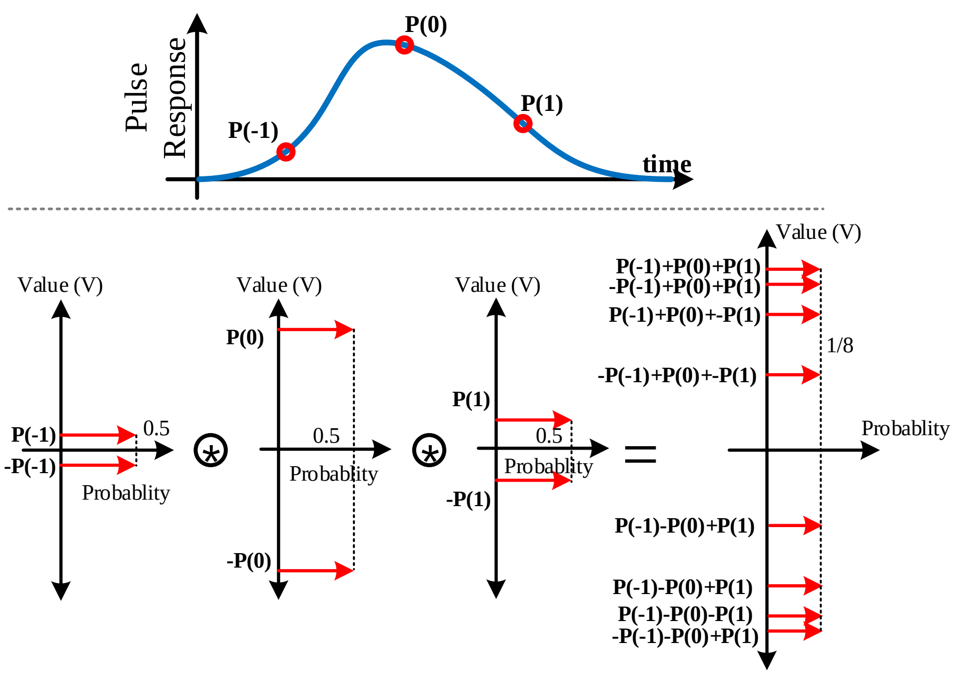

Figure 5 - Graphic representation of calculating PDF from a pulse response

Table 2 shows a summary of the advantages and disadvantages of each of the methods to calculate ICN. In section III, the frequency domain method is used for quick mathematic analysis of the link. In Section IV, a statistical model using time domain method is employed for incorporating the effects of ICN on the system performance.

Table 2 - Summary of the advantages and disadvantages of using a frequency vs time domain method for calculating ICN

Frequency Domain		Time Domain	
	Quickly from S-parameters		Accurately captures actual crosstalk amount
	Method used by standards		Simulation setup slightly more challenging
	May not represent actual crosstalk impact		

III. Link Modelling and Mathematical Analysis

To conduct a mathematical analysis of how ICN can be scaled as the channel insertion loss changes, so that the desired error performance of the link can be preserved, the system model shown in Figure 6 is considered.

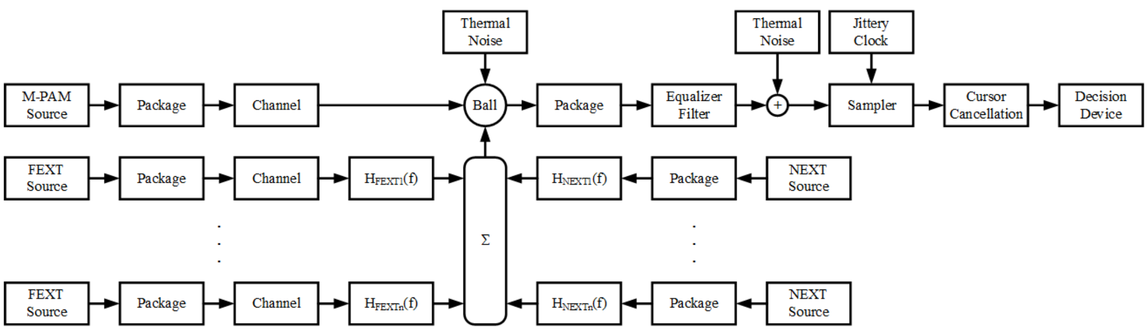

Figure 6 - Link model used for mathematical analysis

The model assumes a signal, generated by an M-level PAM (M-PAM) source, is transmitted with M equally-spaced levels within a peak-to-peak value of $\pm V_S$. The signal passes through a combination of a transmitter package and a transmission channel. A series of aggressors, including NEXTn near-end crosstalk (NEXT) and FEXTn far-end crosstalk (FEXT) interfere with the signal at the input of the receiver (receiver ball). The analysis formulates the tradeoff between tolerable crosstalk, in terms of ICN, and attenuation that the victim signal can undergo, in terms of the channel IL, and still be detectable at a desired performance level. The received signal passes through a receiver package and enters an equalizing filter for dispersion compensation. The combination of an input-referred thermal noise and an after-equalizer thermal noise also contaminates the signal. The equalized signal is then sampled, and after further pre and post ISI cursor cancellation, is presented to a decision device for final detection. Note that with careful consideration, the order of some of the described operations in this model can be changed without affecting the analysis outcome. For example, equalization may be partially moved to the transmitter, or noise may be added elsewhere or even at multiple points.

The model considers the impact of the following impairments, believed to noticeably contribute to the error performance of the link:

a) Residual ISI left from non-ideal equalization
b) Crosstalk contamination from NEXT and FEXT aggressors
c) Thermal noise
d) Timing jitter at the receiver sampler
e) Limited sensitivity of the receiver decision device

In the following sections, we further explain the impairments and assumptions we make to model their impact. The analysis is based on statistical modeling at the input of the receiver decision device as functions of the amount of channel IL at the Nyquist frequency. The ultimate goal is to derive a relationship between ICN and channel Nyquist IL in the presence of the above non-idealities and from there the slope of this relationship.

A. Residual ISI

We assume that the residual ISI is a result of under-equalization of the signal, imposed by various practical limitations and considerations. Given that M symbol levels of the transmitted signal are assumed to be equally likely and independent, the mean of the residual ISI will be zero.

$$V_{ISI,mean} = 0 \tag{7}$$

The std value of the residual ISI can be calculated by a power sum operation over the non-zero pre and post cursors of the pulse response of the link. Obviously, the loss profile of the under-equalized link response is needed to be able to calculate the cursor values. This loss, $H_{link}(s)$, is the result of applying the equalizer filter gain, $H_{eq}(s)$, to the total link attenuation, which is a result of two packages, $H_{pkg(s)}$ each, and the channel, $H_{ch}(s)$. In this analysis, we assume that the link response can be approximated by a skin effect profile plus an additional $-60dB/dec$ attenuation roll-off passed the Nyquist frequency. A skin profile was chosen because it closely resembles reality and is mathematically attractive. The additional $-60dB/dec$ roll-off loss represents the effect of bandwidth limitation of the equalizer filter due to parasitic poles and is modeled by a third-order Butterworth filter, $H_{Butt3}(s)$. In other words, we assume:

$$H_{link}(s) = H_{pkg}{}^2(s)H_{ch}(s)H_{eq}(s) = e^{-K_s\sqrt{s}}H_{Butt3}(s) \tag{8}$$

The skin profile is in turn assumed to be a function of the channel Nyquist IL so that it starts from a known Nyquist under-equalization loss of $Att_{skin,min}$ for zero-loss channel and achieves a known Nyquist under-equalization loss of $Att_{skin,N0}$ for an arbitrarily-chosen reference channel. Noting that at Nyquist frequency $s = 2\pi f_N$, and if subscript N is used to represent quantity values at Nyquist frequency and subscript 0 to represent values for the reference link, then the assumption leads to the following expression for the skin factor, K_s, as a function of the channel Nyquist IL, $|H_{ch,N}|$:

$$K_s(|H_{ch,N}|) = \frac{-1}{\sqrt{\pi f_N}}\left[\frac{ln(|H_{ch,N}|)}{ln(|H_{ch,N0}|)}ln\left(\frac{Att_{skin,N0}}{Att_{skin,min}}\right) + ln(Att_{skin,min})\right] \tag{9}$$

From combining Equations (8) and (9) the following expression for under-equalization loss of the link at the Nyquist frequency results:

$$|H_{link,N}| = |H_{pkg,N}|^2 |H_{ch,N}||H_{eq,N}| = \frac{1}{\sqrt{2}} Att_{skin,min} \left(\frac{Att_{skin,N0}}{Att_{skin,min}}\right)^{\frac{ln(|H_{ch,N}|)}{ln(|H_{ch,N0}|)}} \quad (10)$$

In accordance with the definition of Nyquist frequency, if a pulse with a width of $1/2f_N$ is applied to a system described by the under-equalization response of Equation (8), with K_s given by Equation (9), it produces the following pulse response:

$$h_{link}(t) = \left[erfc\left(\frac{K_s}{2\sqrt{t}}\right) - erfc\left(\frac{K_s}{2\sqrt{t-\frac{1}{2f_N}}}\right)\right] * 2\pi f_N \left(e^{-2\pi f_N t} - \frac{2}{\sqrt{3}} e^{-\pi f_N t} cos\left(\sqrt{3}\pi f_N t + \frac{\pi}{6}\right)\right) \quad (11)$$

This pulse response along with its samples taken by a clock generated by a center-locked clock and data recovery (CDR) unit is plotted in Figure 7 for a 9dB skin-profile under-equalization case.

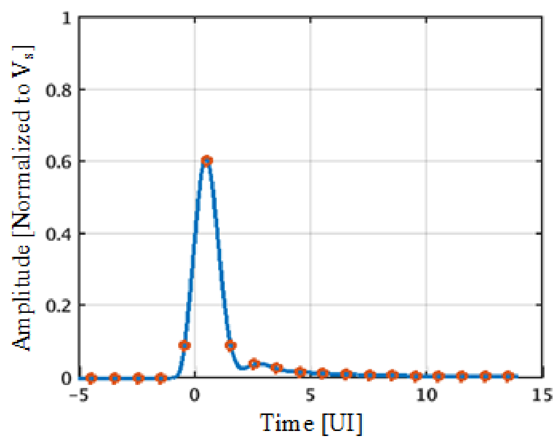

Figure 7 - Pulse response of a 9dB skin-profile under-equalized link

From the shown pre and post ISI samples, the ones that fall outside the window of the proceeding cursor cancellation block, will contribute to the residual ISI impairment. Assuming a window size of N_{pre} for pre-cursor cancellation and a window size of N_{post} for post-cursor cancellation, the std value of the residual ISI can be calculated:

$$V_{ISI,std} = V_s \sqrt{\left(\frac{1}{3}\frac{M+1}{M-1}\right) \sum_{n<-N_{pre}\,\&\,n>N_{post}} h_{link}{}^2\left(\frac{n}{2f_N}\right)} \quad (12)$$

Note that the term inside bracket in this equation reflects averaging operation needed due to M-PAM signaling.

B. Crosstalk

Crosstalk is a result of signal contamination by NEXT and FEXT aggressors. Given that the crosstalk sources are all assumed to use similar M-PAM transmitters with zero averages, plus the usual high-pass nature of the crosstalk signal paths, crosstalk will have a mean of zero:

$$V_{X,mean} = 0 \tag{13}$$

Noting that there is a transfer function from the ball to the input of the receiver decision device due to the combination of a package loss and an equalizer filter gain, we approximate the std value of crosstalk at the input of the receiver decision device by scaling ICN at the ball with the value of this transfer function at the Nyquist frequency. That is:

$$V_{X,std} = |H_{pkg,N}||H_{eq,N}|ICN \tag{14}$$

Equation (14) can be combined with (10) to yield the following estimate for the crosstalk std value at the input of the receiver decision device:

$$V_{X,std} = \frac{Att_{skin,min}}{\sqrt{2}|H_{pkg,N}||H_{ch,N}|}\left(\frac{Att_{skin,N0}}{Att_{skin,min}}\right)^{\frac{ln(|H_{ch,N}|)}{ln(|H_{ch,N0}|)}} ICN \tag{15}$$

For legacy reasons from the original binary NRZ signaling scheme, it is customary to quantify ICN of the M-PAM scheme as if a binary NRZ signaling at a bit rate equal to the M-PAM baud rate and with the same peak-to-peak value was used for aggressors. In this case, it is needed to obtain the relationship between ICN of these two schemes. This can be achieved by applying Equation (1) to an M-PAM signaling scheme. It can be easily shown that in this case the PSD of the transmitted signal can be given by:

$$PSD_{M-PAM} = {V_s}^2\left(\frac{1}{3}\frac{M+1}{M-1}\right)sinc^2\left(\frac{f}{2f_N}\right) \tag{16}$$

which results in the following expression for the ICN of the M-PAM system with M-PAM aggressors:

$$ICN = V_s\sqrt{\left(\frac{1}{3}\frac{M+1}{M-1}\right)\frac{1}{2f_N}\int_{-\infty}^{\infty}\sum_i |H_{X,i}(f)|^2\, sinc^2\left(\frac{f}{2f_N}\right)df} \tag{17}$$

Noting that the ICN of the M-PAM system with legacy binary NRZ aggressor assumption, ICN_{NRZ}, is simply the above equation for $M = 2$, plus the fact that the Nyquist frequency for both cases is the same, results in the following ratio relationship between ICN and ICN_{NRZ}:

$$\frac{ICN}{ICN_{NRZ}} = \sqrt{\frac{1}{3}\frac{M+1}{M-1}} \tag{18}$$

which is simply the ratio between the average powers of the M-PAM and binary NRZ signals. As an example, for $M = 4$, if a binary NRZ aggressor produces $1mV$ of ICN at the receiver ball, an M-PAM aggressor working at the same baud rate and with the same peak-to-peak signal swing will produce $0.75mV$ of ICN. Combining Equations (15) and (18) yields:

$$V_{X,std} = \sqrt{\frac{1}{3}\frac{M+1}{M-1}}\frac{Att_{skin,min}}{\sqrt{2}|H_{pkg,N}||H_{ch,N}|}\left(\frac{Att_{skin,N0}}{Att_{skin,min}}\right)^{\frac{ln(|H_{ch,N}|)}{ln(|H_{ch,N0}|)}} ICN_{NRZ} \quad (19)$$

Equation (19) is an alternative to Equation (15) when the legacy binary NRZ aggressors are assumed to have caused the crosstalk to an M-PAM victim and expresses the crosstalk std value at the input of the receiver decision device as a function of the channel IL at the M-PAM Nyquist frequency and legacy ICN_{NRZ}.

C. Thermal Noise

Thermal noise is modeled by combining two independent components. The first component is the result of the input-referred PSD at the receiver input and the second component is any additional noise that is added after the equalizer filter. Thermal noise usually has a Gaussian distribution with a mean value of zero:

$$V_{N,mean} = 0 \quad (20)$$

Since thermal noise at the input of the receiver decision device is a result of combining the input noise (input-referred noise amplified by the equalizer filter) plus the output noise (additional noise added after the equalizer filter), its std value can be calculated as:

$$V_{N,std} = \sqrt{V_{N,std,input}^{2} + V_{N,std,output}^{2}} = \sqrt{\int_{-\infty}^{\infty} PSD_{noise,input}|H_{eq}(f)|^{2} df + V_{N,std,output}^{2}} \quad (21)$$

Usually, the input-referred thermal noise is white with a constant double-sided PSD of:

$$PSD_{noise,input} = \frac{N_0}{2} \quad (22)$$

Equation (21) describes the general method for calculating the std value of the noise. However, if the integrated noise due to the input-referred noise at the output of the equalizer filter for an arbitrarily-chosen reference link is known (for example, from circuit-level simulations), it can be used to estimate its std value for other channel losses. It is reasonable to assume that the std value of this noise is proportional to the gain of the equalizer filter at the Nyquist frequency. In other words:

$$\frac{V_{N,std,input}}{V_{N,std,input,0}} = \frac{|H_{eq,N}|}{|H_{eq,N0}|} \quad (23)$$

Combining Equation (23) with (10) and (11) results in the following expression that relates the std value of the thermal noise at the input of the receiver decision device to the channel Nyquist IL:

$$V_{N,std} = \sqrt{\left[\frac{|H_{ch,N0}|}{|H_{ch,N}|}\left(\frac{Att_{skin,N0}}{Att_{skin,min}}\right)^{\frac{ln(|H_{ch,N}|)}{ln(|H_{ch,N0}|)}-1} V_{N,std,0}\right]^2 + V_{N,std,output}{}^2} \tag{24}$$

D. Timing Jitter

Jitter is caused by timing perturbations of the CDR unit on the recovered clock that is used to sample the signal in the receiver. For an adequate level of equalization prior to recovering the clock, it is reasonable to assume that jitter is largely independent of the level of equalization and channel IL [2]. Our approach in calculating the effect of timing jitter on the decisions made by the receiver decision device is based on using the inner eye contour as a mapping function between time and voltage domains.

In an M-PAM system, the eye diagram consists of a stack of $M - 1$ separate eye openings. These eye openings are not identical, but similar enough so that for our purpose one inner eye contour can represent all of them. In addition, deriving the time-to-voltage mapping function does not require presence of the impairments so that ideal conditions can be assumed. Figure 8 shows eye diagrams of binary NRZ and 4-PAM schemes under these conditions. In this figure, single-tone Nyquist components that create the inner eye contours and act as the mapping functions are highlighted in red. Furthermore, exemplary regions of the contours that the mapping function operates on are highlighted in thick red.

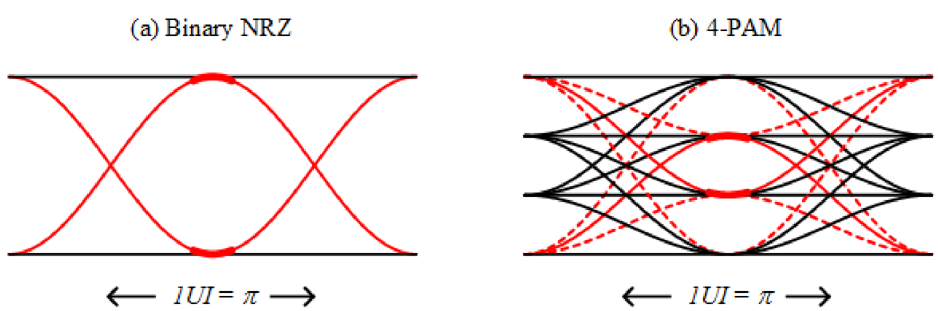

Figure 8 - Binary NRZ (a) and 4-PAM (b) eye diagrams under ideal conditions

As can be seen, the three stacked inner eye contours of the 4-PAM case are slightly different. We choose to use the middle eye inner contour, highlighted in solid red, for the purpose of deriving the mapping function for this case. Generalization of this approach to M-PAM and considering the transmitted peak-to-peak value of $\pm V_s$ and under-equalization assumption at the Nyquist frequency given by Equation (10), results in the following expression for the mapping function at the input of the receiver decision device:

$$f_{map}(x) = \frac{V_s|H_{link,N}|}{2}\frac{M}{M-1}\left(cos(x) - \frac{M-2}{M}\right) \tag{25}$$

Note that for cases of odd M there will be no middle eye, nevertheless, the above expresses can continue to be used for our purposes.

Timing jitter that the mapping function operates on is a random variable and can be described by its PDF, $f_X(x)$. It can be shown that transformation of this PDF by the mapping function of Equation (25) results in the following PDF [3]:

$$f_Y(y) = \frac{f_X\left(cos^{-1}\left(\frac{2y}{V_s|H_{link,N}|}\frac{M-1}{M}+\frac{M-2}{M}\right)\right)+f_X\left(-cos^{-1}\left(\frac{2y}{V_s|H_{link,N}|}\frac{M-1}{M}+\frac{M-2}{M}\right)\right)}{\sqrt{\left(\frac{V_s|H_{link,N}|}{2}\frac{M}{M-1}\right)^2-\left(y+\frac{V_s|H_{link,N}|}{2}\frac{M-2}{M-1}\right)^2}} \quad ,0 \le y \le \frac{V_s|H_{link,N}|}{M-1} \qquad (26)$$

In deriving Equation (26), its domain has been calculated from the transformation of the domain of the timing jitter, which is the horizontal opening of the inner eye contour given by the following expression:

$$f_X(x) \quad ,-cos^{-1}\left(\frac{M-2}{M}\right) \le x \le cos^{-1}\left(\frac{M-2}{M}\right) \qquad (27)$$

Transformation of timing jitter to voltage domain by the mapping function is graphically illustrated in Figure 9(a).

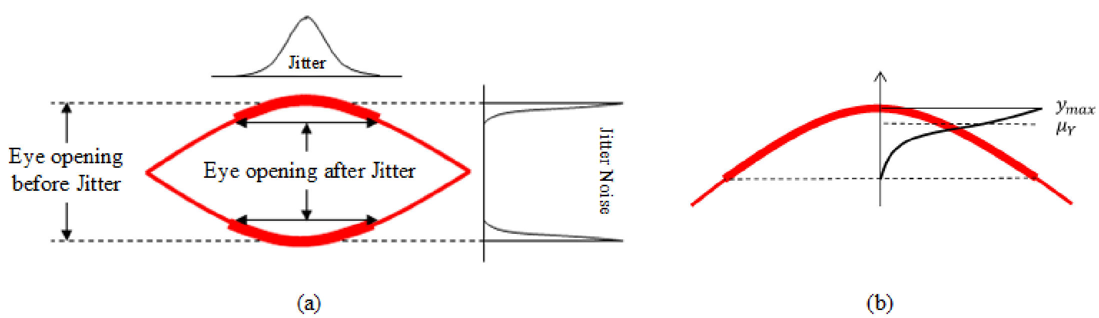

Figure 9 - (a) Transformation of jitter from time domain to voltage domain (b) Average eye closure from the top side

The mean and std values of random variable Y, namely μ_Y and σ_Y, can be calculated from its PDF and used to calculate the mean and std values of the jitter noise. Note that even if the timing jitter has a zero mean, the jitter noise will have a non-zero mean. This is due to the nature of the mapping function that generates a one-sided output from its two-sided input, as illustrated in Figure 9(a). To calculate this value, we note that the average amount of eye closure from each side is equal to the voltage drop from the maximum point of the eye opening (corresponding to maximum value of Y) to the mean level of Y. This is shown in Figure 9(b) for the top side of the inner eye of Figure 4(a). This, in combination with Equation (10), leads to the following expression for the mean value of the jitter noise:

$$V_{J,mean} = \frac{\sqrt{2}V_s}{M-1}Att_{skin,min}\left(\frac{Att_{skin,N0}}{Att_{skin,min}}\right)^{\frac{ln(|H_{ch,N}|)}{ln(|H_{ch,N0}|)}} - 2\mu_Y \qquad (28)$$

The std value of the jitter noise can be calculated by multiplying the std value of variable Y by $\sqrt{2}$. This is due to independent closure of the eye from both vertical sides. Independent closure is a result of eye sampling at different UI time steps. As a result:

$$V_{J,std} = \sqrt{2}\sigma_Y \tag{29}$$

E. Receiver Sensitivity

Receiver sensitivity is simply modeled as considering an additional margin, V_{sen}, for the opening of the eye at the input of the receiver decision device, so that decisions can be made unambiguously. As a result:

$$V_{S,mean} = V_{sen} \tag{30}$$

Since this margin is assumed to be fixed:

$$V_{S,std} = 0 \tag{31}$$

Once the impairments are modeled, we can start formulating the condition for having an open eye. Under an impairment-free condition, a stack of $M - 1$ of such eye openings should fit in the peak-to-peak span of the signal at the input of the receiver decision device. Addition of the impairments at this point results in a random number with a mean value equal to the sum of the mean values and a std value obtained from root-square summation of the std values. While the impact of the mean value is a direct reduction in the eye opening, the impact of the std value will depend on the desired error performance level of the link. Since the overall impairment is a result of contribution from several independent random components, it is reasonable to assume that the rule of Gaussian scaling applies. This rule relates the maximum value that a Gaussian variable can take with a desired probability to its std value and is often calculated from the Q function [4]. Figure 10 shows a plot of this scaling factor as well a table for some typical data points.

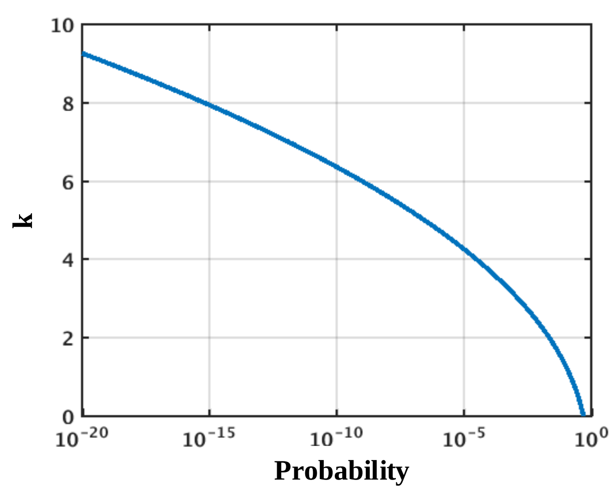

Probability	k
1e-3	3.09
1e-4	3.72
1e-5	4.26
1e-6	4.75
1e-7	5.20
1e-8	5.61
1e-9	6.00
1e-10	6.36
1e-11	6.71
1e-12	7.03
1e-13	7.35
1e-14	7.65
1e-15	7.94
1e-16	8.22
1e-17	8.49
1e-18	8.76

Figure 10 - Gaussian distribution std to peak scaling rule

The performance of the M-PAM scheme is often expressed in terms of its bit errors, not symbol errors. As a result, before the BER is translated to the std scaling factor, it needs to be converted to the M-PAM symbol-error rate (SER). If Gray coding is used to map the binary bits into M-PAM symbols, each symbol error results in only one bit error. As a result, the following relationship can be used to relate BER to SER:

$$SER = log_2(M)BER \tag{32}$$

The requirement of having an open eye is that the impairment-free eye opening should be large enough to accommodate the closure contributed by the combination of all impairments. The boundary condition of this requirement, written at the input of the receiver decision device expresses that:

$$\frac{2V_s}{M-1}\left|H_{link,N}\right| = \left(V_{ISI,mean} + V_{X,mean} + V_{N,mean} + V_{J,mean} + V_{S,mean}\right) + 2k(SER)\sqrt{{V_{ISI,std}}^2 + {V_{X,std}}^2 + {V_{N,std}}^2 + {V_{J,std}}^2 + {V_{S,std}}^2} \tag{33}$$

All the terms involved in this expression were calculated in the above sections in terms of constant system parameters and variable parameters ICN_{NRZ} (or ICN) and $\left|H_{ch,N}\right|$. The derivative of this equation with respect to $\left|H_{ch,N}\right|$ expresses the slope of ICN versus channel Nyquist IL. It is of our particular interest to express the slope relationship in logarithmic scale. That is the slope of ICN versus link Nyquist IL in dB, defined as:

$$IL = -20log_{10}\left(\left|H_{pkg,N}\right|^2\left|H_{ch,N}\right|\right) \tag{34}$$

which can be used to relate the slopes in linear and logarithmic scale.

Figure 11 shows the results of the analysis for a set of constant parameters of an exemplary link with IL ranging from $5dB$ to $25dB$. Both ICN and its slope are plotted versus the total (bump-to-bump) link Nyquist IL in logarithmic scale.

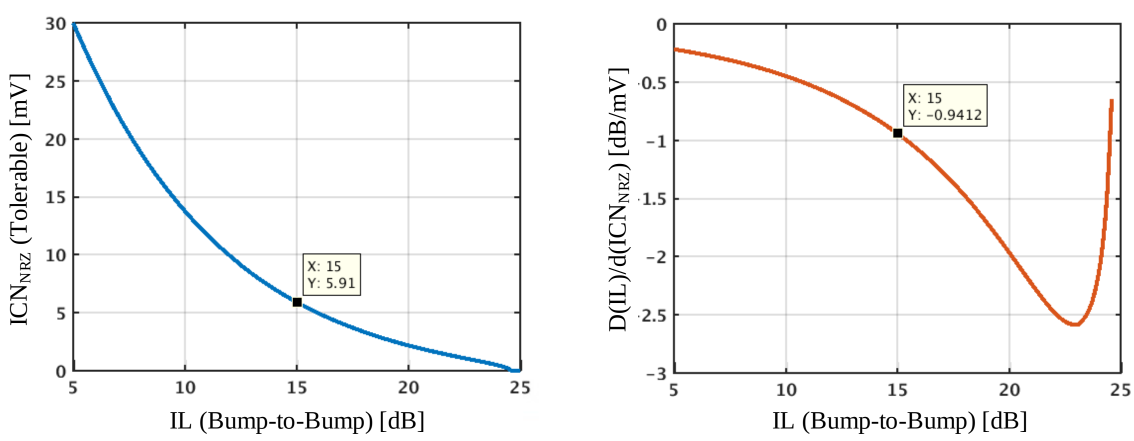

Figure 11 - Calculated ICN and ICN slope plots for the link example

This figure suggests that for this link, for example, at a 15dB of bump-to-bump link loss a legacy binary NRZ ICN of up to 5.9mV is tolerable to achieve the BER target. It also suggests that at this operating condition, if ICN is increased/decreased by 1mV, 0.94dB less/more Nyquist IL can be tolerated. The system parameter assumptions for the above example are the same as those used in the next section, where a more elaborate analysis based on the statistical eye analysis will be presented.

Further examination of this example, highlighted by the change in the behavior of the ICN slope at higher losses, reveals that while for low loss channels crosstalk dominates the performance, at high loss thermal noise dominates. Figure 12 shows the std deviation of these two impairments at the decision point as the IL changes, clearly illustrating this crossover behavior. This crossover behavior is intuitively expected since as loss increases, the equalizer filter applies more gain and enhances the noise, leaving less margin to tolerate crosstalk. The crossover manifests itself in the slope plot of Figure 11, in the way the slope varies in its vicinity.

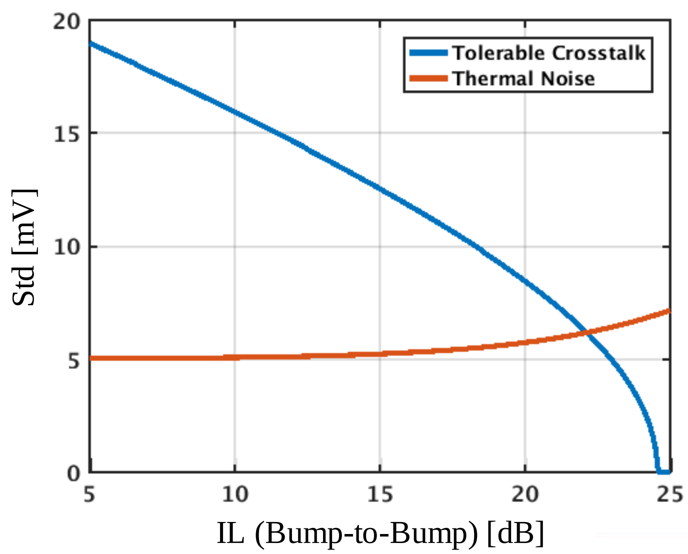

Figure 12 - Crossover between tolerable crosstalk and thermal noise at the decision point

IV. Link Statistical Simulations

In this section, a statistical model is used to determine the ICN vs. loss performance of a very short-reach (VSR) link. The link is operating at 56Gb/s and uses a 4-PAM modulation scheme. In the model, the signal PDF is generated from the pulse response of the ISI. The exact same procedure that was explained in section II.B is applied to the pulse response of ISI. The crosstalk PDF along with other noise sources are convolved with the ISI PDF to determine the overall signal PDF, giving a more accurate picture of the crosstalk. The receiver non-linearity is also included by compressing the overall PDF. Furthermore, timing impairments are added to model other non-idealities in the system. After all impairments are included, a statistical eye can be generated for the system which shows the eye opening at different BERs as shown in Figure 13. To determine the maximum tolerable ICN, the amount of crosstalk is increased until the statistical eye opening reaches the receiver sensitivity as the desired BER. In this analysis, a receiver sensitivity of 10mV is used at a BER of 1E-6.

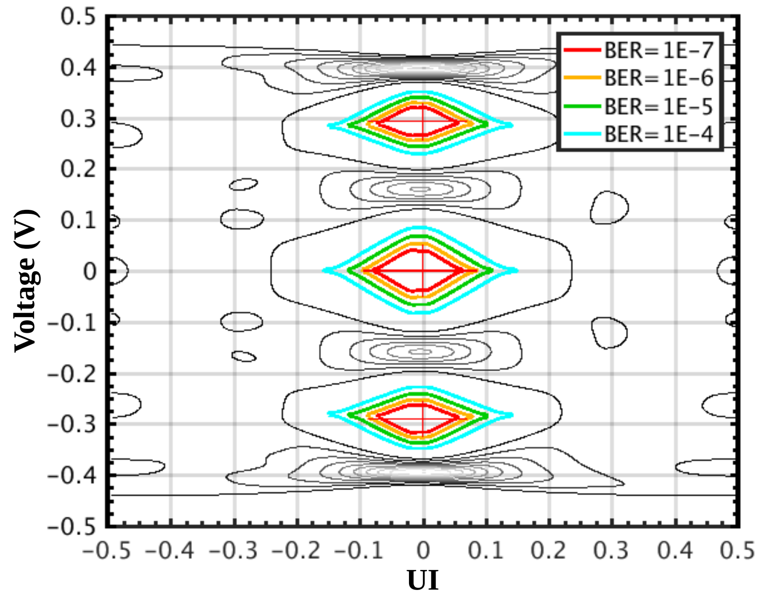

Figure 13 - Statistical eye diagram after including all impairments

Figure 14 shows the maximum tolerable ICN at the ball for different insertion losses. The results of the statistical simulations and mathematical model are both shown. The main reasons for the differences in the two results are the additional non-idealities that the statistical model considers as well as more elaborate representation of the impairments during the statistical simulation than what the mathematical analysis assumes. Nevertheless, both approaches show a similar trend with similar IL vs ICN slope.

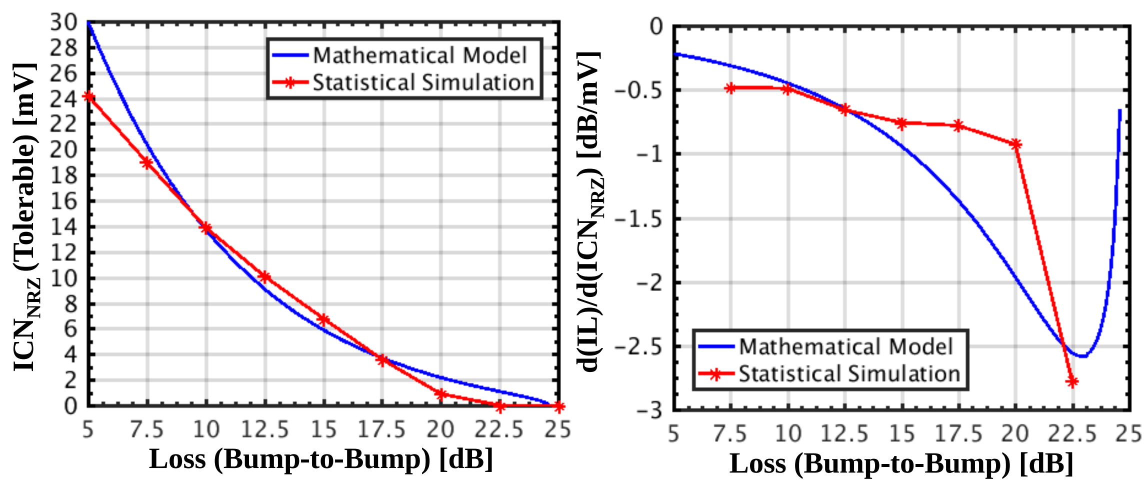

Figure 14 - IL vs ICN and ICN slope comparing mathematical model and statistical simulations

V. Conclusion

This paper outlined the emerging metric of ICN vs. loss to characterize a wireline link performance. The advantages and disadvantages of reporting ICN at the ball vs. bump were summarized. Two different methodologies were provided for calculating ICN in time and frequency domains, with their advantages and disadvantages outlined. A mathematical framework was developed and presented to allow for calculating the ICN tolerance vs. IL and the ICN vs. IL slope without needing detailed information about the system components. This mathematical analysis was compared to the more elaborate statistical model simulations. Using the ICN vs. loss and the slope can help characterize the complete system performance as well as the link sensitivity to changes in both IL and ICN.

VI. References

[1] Optical Internetworking Forum, "OIF-CEI-04.0 (Common Electrical I/O (CEI) - Electrical and Jitter Interoperabilityagreements for 6G+bps, 11G+bps, 25G+bps I/O and 56G+ bps)," 2017.

[2] F. Rao and S. Hindi, "Frequency domain analysis of jitter amplification in clock channels," *IEEE 21st Conference on Electrical Performance of Electronic Packaging and Systems*, pp. 51-54, 2012.

[3] Z. Peyton and J. Peebles, Probability, Random Variables, And Random Signal Principles, vol. 32, McGraw-Hill, 1980.

[4] J. G. Proakis and M. Salehi, "Digital Communications," vol. 27, McGraw-Hill, 5th Edition, 2008.